



## Potential improvements in brain dose estimates for internal emitters

Richard W. Leggett, Sergei Y. Tolmachev & John D. Boice Jr.

To cite this article: Richard W. Leggett, Sergei Y. Tolmachev & John D. Boice Jr. (2018): Potential improvements in brain dose estimates for internal emitters, International Journal of Radiation Biology, DOI: [10.1080/09553002.2018.1554923](https://doi.org/10.1080/09553002.2018.1554923)

To link to this article: <https://doi.org/10.1080/09553002.2018.1554923>



Accepted author version posted online: 04 Dec 2018.  
Published online: 11 Jan 2019.



Submit your article to this journal [↗](#)



Article views: 7



View Crossmark data [↗](#)

ORIGINAL ARTICLE



## Potential improvements in brain dose estimates for internal emitters

Richard W. Leggett<sup>a</sup>, Sergei Y. Tolmachev<sup>b</sup> and John D. Boice, Jr.<sup>c,d</sup>

<sup>a</sup>Oak Ridge National Laboratory, Oak Ridge, TN, USA; <sup>b</sup>U.S. Transuranium and Uranium Registries, College of Pharmacy and Pharmaceutical Sciences, Washington State University, Richland, WA, USA; <sup>c</sup>National Council on Radiation Protection and Measurements, Bethesda, MD, USA; <sup>d</sup>Division of Epidemiology, Department of Medicine, Vanderbilt Epidemiology Center and Vanderbilt-Ingram Cancer Center, Nashville, TN, USA

### ABSTRACT

**Background:** Element-specific biokinetic models are used to reconstruct doses to systemic tissues from internal emitters. Typically, a systemic model for a radionuclide explicitly depicts only its dominant repositories. Remaining tissues and fluids are aggregated into a pool called *Other tissue* in which the radionuclide is assumed to be uniformly distributed. In the systemic biokinetic models used in radiation protection, the brain usually is addressed as an implicit mass fraction of *Other tissue* rather than an explicitly depicted repository. Due to increasing interest in radiation effects on the brain, efforts are underway to improve brain dosimetry for internal radiation sources.

**Methods:** We assessed potential improvements in brain dosimetry for internal emitters by explicitly modeling brain kinetics rather than treating the brain as a mass fraction of *Other tissue*. We selected 10 elements for which brain kinetics can be modeled using published biokinetic data. Injection dose coefficients were calculated for a relatively long-lived radioisotope of each element using each of two versions of the ICRP's latest systemic biokinetic model for the element, the original version and a modified version differing only in the treatment of brain. If the ICRP model contained an explicit brain pool, the modified version depicted brain instead as a mass fraction of *Other tissue*. If the ICRP model included brain in *Other tissue*, the modified version included an explicit brain pool with kinetics based on best available brain-specific data.

**Results:** The result for a given radionuclide is expressed as a ratio A:B, where A and B are the dose coefficients based on the versions of the model with and without an explicit brain pool, respectively. The following ratios A:B were obtained for the 10 radionuclides addressed here: <sup>241</sup>Am, 0.13; <sup>207</sup>Pb, 0.57; <sup>234</sup>U, 0.81; <sup>239</sup>Pu, 0.96; <sup>203</sup>Hg (vapor), 1.4; <sup>134</sup>Cs, 1.5; <sup>54</sup>Mn, 1.7; <sup>210</sup>Po, 1.7; <sup>226</sup>Ra, 1.9; <sup>210</sup>Pb, 3.3. These ratios indicate that a dose estimate for brain based on a biokinetic model with brain implicitly contained in *Other tissue* may substantially underestimate or substantially overestimate a dose estimate that reflects best available brain-specific biokinetic data. Of course, the reliability of the latter estimate depends on the quality of the underlying biokinetic data.

**Conclusions:** Where feasible, the brain should be depicted explicitly in biokinetic models used in epidemiological studies addressing adverse effects of ionizing radiation.

### ARTICLE HISTORY

Received 10 September 2018  
Revised 20 November 2018  
Accepted 21 November 2018

### KEYWORDS

Radiation dose;  
reconstruction; biokinetics;  
brain; epidemiology

## Introduction

There is an increasing interest in potential adverse effects of ionizing radiation on the brain. For example, the Million Person Study (MPS) is evaluating dementia as well as more specific brain diseases such as Alzheimer's, Parkinson's, and motor neuron disease as possible adverse outcomes of combined high- and low-LET exposures to brain tissue (Boice 2017; Boice et al. 2018). The National Aeronautics and Space Administration (NASA) is evaluating the level of protection needed against in-flight behavioral and cognitive impairments from galactic cosmic rays (GCRs). NASA is interested in epidemiological findings on alpha-particle dose to brain as a limited analogy that might inform their decisions regarding protection against the high-energy charged particles encountered in space (NCRP 2016; Boice 2017).

Element-specific biokinetic models are used to reconstruct doses to systemic tissues from internal emitters. These

models typically depict explicitly only those tissues that tend to dominate the systemic behavior of the element over time. The remaining tissues are aggregated into a pool called *Other tissue* in which activity is assumed to be uniformly distributed. Explicitly identified tissues usually consist of some subset of liver, kidneys, bone, bone marrow, gonads, thyroid, spleen, and skin. The brain is included explicitly in systemic biokinetic models for a few elements but typically is addressed as an implicit mass fraction of *Other tissue*.

This paper assesses potential improvements in brain dosimetry for internal emitters from explicit modelling of brain kinetics rather than treating the brain as an implicit mass fraction of *Other tissue*. The analysis serves more generally as a case study of potential errors in radiation dose estimates resulting from assuming common biokinetics and uniform activity concentration across a large collection of tissues with different compositions and physiological functions. Comparisons are made of dose coefficients for selected

radionuclides based on alternate versions of the systemic biokinetic model for each radionuclide, differing only with respect to explicit versus implicit treatment of brain tissue.

## Methods

Biokinetic data for elements are considerably more limited for brain than for tissues, such as bone, liver, and kidneys, that are commonly addressed explicitly in the biokinetic models used in radiation protection and dose reconstruction for radionuclides. Typically, quantitative data on uptake and retention of a given element by the brain come primarily from a small number of studies on laboratory animals. Thus, the explicit models for brain considered in the present study generally rely heavily on data for laboratory animals, mixed with available relevant information for humans such as autopsy measurements indicating the relative contents of an element in the brain and other tissues. The reader is referred to an article by Leggett (2001) for a critical examination of the basis for interspecies extrapolation of biokinetic data, the sources and extent of uncertainties inherent in such extrapolation, and the animal species that have proven to be the most reliable laboratory models for human biokinetics of different families of elements.

We selected 10 radionuclides for which informative element-specific data are available on relative levels of accumulation by the brain and other systemic repositories. Half of these radionuclides are included because they are important internal emitters encountered in the MPS:  $^{210}\text{Po}$  (Boice et al. 2006, 2014),  $^{226}\text{Ra}$  (Silver et al. 2013; Ellis et al. 2018),  $^{234}\text{U}$  (Boice et al. 2006; Ellis et al. 2018),  $^{239}\text{Pu}$  (Gilbert et al. 1993; Wiggs et al. 1994; Boice et al. 2014), and  $^{241}\text{Am}$  (Boice et al. 2006). Four other radionuclides,  $^{54}\text{Mn}$ ,  $^{134}\text{Cs}$ ,  $^{203}\text{Hg}$  (inhaled as a vapor), and  $^{210}\text{Pb}$ , are included as convenient case studies for exploring the value of an explicit brain model for estimating doses to brain because a well-founded brain model already existed for each of these elements. The remaining radionuclide,  $^{207}\text{Bi}$ , illustrates a situation that may frequently arise in assessing the usefulness of an explicit brain model, that is, data on brain kinetics of the element are available but of questionable relevance for modeling biokinetics in humans.

For each of the 10 radionuclides, we compared alternate dose coefficients for brain, one based on the ICRP's latest systemic model for the element and the other based on a modification of that model with a different treatment of brain as described below. Two different variations of the ICRP model were considered for  $^{210}\text{Po}$ . It was assumed that the radionuclide is injected into blood of a male worker. The ICRP's updated dosimetry system for workers (ICRP 2016a) was applied.

If the ICRP model for the element already contained an explicit brain pool, a modified version of the ICRP model was constructed by removing the brain pool so that brain was included implicitly in *Other tissue*. The deposition fractions (fractional outflows from a central blood compartment to specified destinations) for compartments of *Other tissue* were increased proportionally so that the sum of the new deposition fractions for compartments of *Other tissue* equaled the

sum of all deposition fractions for the brain and *Other tissue* in the ICRP model. Suppose, for example, that in the ICRP model the deposition fraction for the brain is 0.006 and that *Other tissue* contains two compartments with deposition fractions 0.1 and 0.2. In the alternate model, the deposition fractions for the two compartments of *Other tissue* would be increased to  $0.1 + 0.002 = 0.102$  and  $0.2 + 0.004 = 0.204$ .

If the brain was implicitly contained in *Other tissue* in the ICRP model for the element, then a modified version of the ICRP model was constructed by adding an explicit brain pool that exchanged activity with blood and assigning transfer coefficients between brain and blood based on brain-specific biokinetic data. If needed, the deposition fractions for compartments of *Other tissue* were decreased proportionally so that the sum of all deposition fractions for *Other tissue* and the brain equaled the sum of the deposition fractions for compartments of *Other tissue* in the ICRP model. Such an adjustment was not needed if the blood compartment feeding the added brain compartment(s) was not directly connected to *Other tissue*.

## Results

### Polonium

The analysis for  $^{210}\text{Po}$  is described in some detail to illustrate the general approach used here and the considerations that went into selection of biokinetic data.

The ICRP's latest model for systemic polonium (Po) is described in Publication 137 (2017), the third part of a series of reports that provide models, dose coefficients, and reference bioassay data for assessment of occupational exposure to radionuclides (the 'OIR' series). A more detailed description of the basis for the model is given in an article by Leggett and Eckerman (2001). The structure of the model is shown in Figure 1. Transfer coefficients for a reference

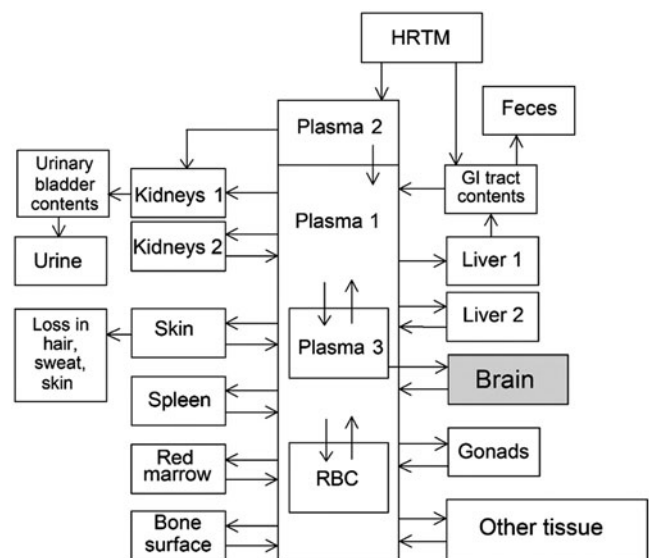


**Figure 1.** Model structure for systemic Po. The unshaded boxes and associated arrows represent the ICRP's latest model (ICRP 2017). The modified version of the ICRP model considered here adds the brain compartment and associated arrows. RBC: red blood cells; HRTM: Human Respiratory Tract Model (ICRP, 2015).

**Table 1.** Transfer coefficients in the ICRP's model for systemic polonium.

From	To	Transfer coefficient ( $d^{-1}$ )
Plasma 2	Plasma 1	800
Plasma 2	Kidneys 1	200
Plasma 1	Plasma 3	4
Plasma 1	RBC	6
Plasma 1	Liver 1	17.5
Plasma 1	Liver 2	17.5
Plasma 1	Kidneys 1	5
Plasma 1	Kidneys 2	5
Plasma 1	Skin	5
Plasma 1	Red Marrow	4
Plasma 1	Bone Surface	1.5
Plasma 1	Spleen	2
Plasma 1	Testes	0.1
Plasma 1	Ovaries	0.05
Plasma 1	Other	32.35
Plasma 3	Plasma 1	0.099
RBC	Plasma 1	0.099
Liver 1	GI Tract	0.139
Liver 2	Plasma 1	0.099
Kidneys 1	Urinary bladder content	0.173
Kidneys 2	Plasma 1	0.099
Skin	Plasma 1	0.00693
Skin	Excreta	0.00693
Red Marrow	Plasma 1	0.099
Bone Surface	Plasma 1	0.0231
Spleen	Plasma 1	0.099
Testes or Ovaries	Plasma 1	0.0139
Other	Plasma 1	0.099

RBC: Red blood cells.

worker are listed in Table 1. The brain is not depicted explicitly in the model and hence is contained implicitly in the single compartment representing *Other tissue*.

The ICRP's model for Po was based to a large extent on data for human subjects exposed to  $^{210}\text{Po}$ , but data for laboratory animals were used to fill sizable gaps in data for humans. Data for baboons and dogs were given higher weight than findings for other studied animals due to the relatively detailed information available for baboons and dogs; quantitative similarities in the distribution and retention of Po in humans, baboons, and dogs; and the general consideration that primates and dogs have proven to be reasonably good laboratory models for human biokinetics of many elements (Leggett 2001). For the same reasons, data for baboons were used here to develop a modified version of the ICRP's model for Po that contains an explicit brain model. The brain was not addressed in the dog studies used in development of the ICRP's model for Po.

Autopsy data on the distribution of  $^{210}\text{Po}$  in tissues are available for uranium miners (Blanchard and Moore 1971) but are not useful for modeling brain kinetics of  $^{210}\text{Po}$  because much of the  $^{210}\text{Po}$  in tissues of these subjects probably arose from radionuclides that sequentially decayed to  $^{210}\text{Po}$  *in vivo*. Polonium-210 was measured at autopsy in an adult male who died 23 days after being poisoned with  $^{210}\text{Po}$  (Nathwani et al. 2016; Harrison et al. 2017). The kidneys showed the highest activity concentration. The activity concentration in brain ( $5500\text{Bq g}^{-1}$ ) was about 10% of that in the kidneys, 20% of that in the liver, and 50% of that in the spleen. The concentration in brain was considerably higher than in muscle. Data for this subject were not used in the derivation of a biokinetic model for brain due to the distinct possibility of a substantially increased level of entry of  $^{210}\text{Po}$

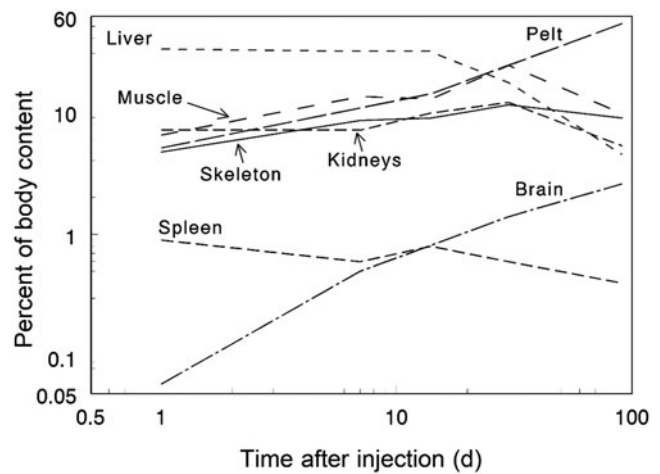


**Figure 2.** Relative  $^{210}\text{Po}$  content in tissues of baboons as a function of time after intravenous injection (data from Cohen et al. 1989; Fellman et al. 1994).

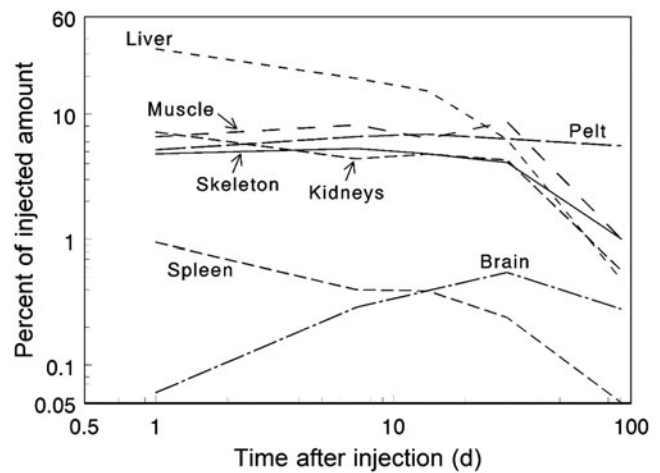


**Figure 3.** Retention on Po in baboon tissues as a function of time after intravenous injection of  $^{210}\text{Po}$  (data of Cohen et al. 1989; Fellman et al. 1994).

into brain resulting from alpha-particle breakdown of the blood-brain barrier.

Following intravenous administration of  $^{210}\text{Po}$  to baboons, the activity concentration was substantially lower in the brain than in other studied tissues over the first week (Cohen et al. 1989, Fellman et al. 1994). The brain content as a fraction of total-body content of  $^{210}\text{Po}$  increased monotonically over the 3-month study period (Figure 2). The data indicate that the residence time for Po in the brain was substantially greater than in other tissues except pelt (Figures 2 and 3).

A variation of the structure of the ICRP's systemic model for Po in workers was developed by addition of a single compartment representing the brain (shaded box in Figure 1). Transfer coefficients describing exchange of Po between brain and compartments of plasma were set to approximate the time-dependent retention of  $^{210}\text{Po}$  in brain determined in the study on baboons summarized above (Figure 4, solid curve). A slow-release blood pool (Plasma 3 in Figure 1) was selected as the feed to brain because of the low rate of accumulation of  $^{210}\text{Po}$  into brain observed in the baboon studies. The following transfer coefficients were added to the set of transfer coefficients listed in Table 1. These transfer

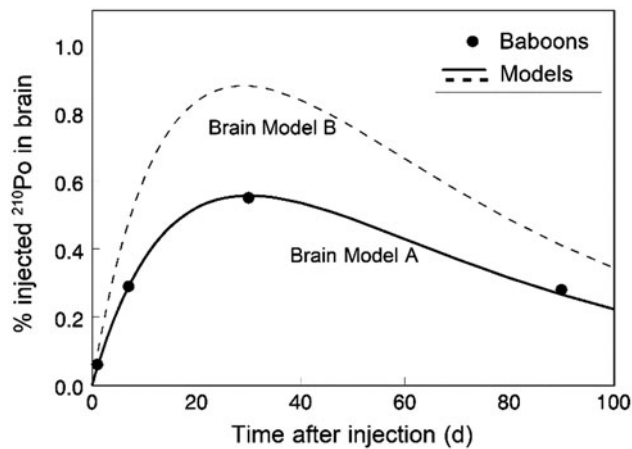


Figure 4. Predictions of brain retention of Po based on two variations of the ICRP's systemic model with different brain kinetics (Brain Model A and Brain Model B defined in text).

coefficients, which were derived from the fit to brain retention data for baboons, are referred to in Figure 4 as Brain Model A:

$$\begin{aligned}\text{Plasma 3 to Brain} &= 0.0135 \text{ d}^{-1}, \\ \text{Brain to Plasma 1} &= 0.0385 \text{ d}^{-1}.\end{aligned}$$

A different variation of the ICRP's Po model was also considered in view of the total reliance of the parameter values for the brain compartment on data for a nonhuman species. The mass of the brain relative to total-body mass appears to be roughly 70% higher for adult humans than adult baboons, based on comparison of data of Cohen et al. (1989) for baboons with data of ICRP Publication 89 (2002) for reference adult humans. It was considered that extrapolation of brain kinetics of Po from baboons to humans should perhaps reflect that difference through assignment of a larger deposition fraction to brain than derived from the baboon data. An alternate modification of the ICRP model was performed by assigning a deposition fraction to brain that is 1.7 times the deposition fraction in Brain Model A. The removal rate from brain to blood was left at the value assigned in Brain Model A. This second set of parameter values for brain is referred to in Figure 4 as Brain Model B:

$$\begin{aligned}\text{Plasma 3 to Brain} &= 0.02295 \text{ d}^{-1}, \\ \text{Brain to Plasma 1} &= 0.0385 \text{ d}^{-1}.\end{aligned}$$

Dose coefficients for brain were derived for injection of  $^{210}\text{Po}$  into blood of a male worker, using the current ICRP model for Po and each of the two modifications of the ICRP model described above, i.e., using Brain Model A or Brain Model B. The dose coefficient based on the modification of the ICRP model using Brain Model A is 1.3 times the value based on the ICRP model. The dose coefficient based on the modification of the ICRP model using Brain Model B is 2.0 times the value based on the ICRP model.

### Bismuth

The ICRP's current systemic model for bismuth (Bi) is described in ICRP Publication 137 (2017). The model structure is shown in Figure 5. Parameter values for an adult

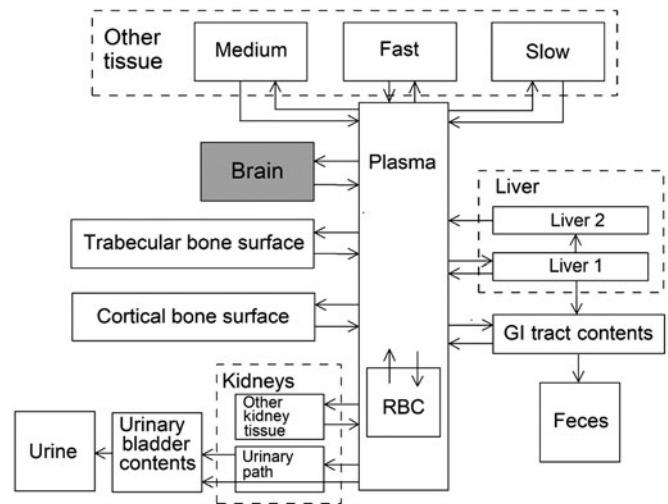


Figure 5. Model structure for systemic Bi. The unshaded boxes and associated arrows represent the ICRP's latest model (ICRP2017). The modified version of the ICRP model considered here adds the brain compartment and associated arrows. RBC: red blood cells; GI: gastrointestinal.

worker are listed in the section on bismuth in Publication 137. In the model, the brain is implicitly contained in *Other tissue*, which consists of three compartments representing fast, medium, and slow phases of removal of Bi to blood.

Autopsy measurements on patients who had received intramuscular Bi treatments indicate the following central estimates of the relative Bi concentrations in tissues: kidney, 1.0; liver, 0.2; spleen, 0.048; colon, 0.039; lung, 0.027; brain, 0.018; blood, 0.015 (Sollmann and Seifter 1942; Sollmann 1957; Fowler and Vouk 1986). The patients apparently lived for extended periods following the end of Bi treatment. The findings suggest relatively low accumulation of Bi by the human brain compared with the other studied tissues.

Biokinetic data for Bi in rats indicate a lower rate of uptake but a longer retention time for Bi in brain than in other soft tissues. In the first few days after parenteral injection of Bi compounds into rats, the brain showed considerably lower uptake of Bi than other tissues (Gregus and Klaassen 1986; Zidenberg-Cherr et al. 1987). Following oral administration of Bi to rats over a 14-month period, the Bi concentration in brain was of the same order as that of most other studied tissues with the main exception of kidneys, the primary repository for Bi (Lee et al. 1980).

A variation of the structure of the ICRP's systemic model for Bi in workers was developed by addition of a compartment representing the brain that exchanges Bi with blood plasma (Figure 5). Parameter values for brain were set for reasonable consistency with the semi-quantitative data on brain kinetics of Bi in human subjects (the times between Bi treatments and death were not found in reports of these studies) and the quantitative data for rats. It was assumed that the brain receives 0.01% of outflow from plasma and loses Bi to plasma with a biological half-time of 100 d. The implied transfer coefficients describing exchange of Bi between plasma and brain are

$$\begin{aligned}\text{Plasma to Brain} &= 0.04 \text{ d}^{-1}, \\ \text{Brain to Plasma} &= 0.00693 \text{ d}^{-1}.\end{aligned}$$



The total outflow rate from plasma to all destinations combined was left unchanged by reducing the transfer coefficients from plasma to each of the compartments of *Other tissue* proportionally to their values in the ICRP model.

Alternate dose coefficients for brain were derived for the case of injection of the long-lived bismuth radioisotope  $^{207}\text{Bi}$  into blood of a male worker, using the current ICRP model for Po and the modification of the ICRP model described above. The dose coefficient based on the modified ICRP model with an explicit brain compartment is 0.57 times the value based on the ICRP model.

## Lead

The ICRP's current systemic model for lead (Pb) is described in ICRP Publication 137 (2017). In this model, the brain is implicitly contained in *Other tissue*, which consists of three compartments representing fast, medium, and slow phases of removal of Pb to blood.

The ICRP's model for Pb is a modified version of a model developed by Leggett (1993) for application to Pb as a chemical hazard as well as a radiation source. The brain was addressed explicitly in the original model because of the brain's sensitivity to Pb as a chemical toxin.

The distribution of Pb in the brain is uneven and varies with the level of exposure. For low-level exposure, the Pb concentration in different regions of the human brain appears to be associated with the potassium concentration, suggesting accumulation of Pb in cell-rich parts of the brain such as the hippocampus (Grandjean 1978; Bryce-Smith and Stephens 1983; Petit et al. 1983). For high exposure, Pb may gain substantial access to neural tissue following breakdown of the blood brain barrier (Petit et al. 1983).

Due to limitations in available region-specific biokinetic data, the brain was represented in the original model (Leggett 1993) as a single compartment that exchanges Pb slowly with a compartment representing diffusible Pb in blood plasma. Parameter values describing the kinetics of Pb in brain were selected for consistency of model predictions with short- to intermediate-term data for laboratory animals including baboons and dogs (Cohen et al. 1970; Lloyd et al. 1975) and autopsy data for Pb in tissues of occupationally or environmentally exposed persons (Leggett 1993).

A modified version of the ICRP's model for systemic Pb was developed by adding a compartment representing brain and assigning flow rates between plasma and brain consistent with predictions of the more detailed model of Leggett (1993). That is, the parameter values describing uptake and outflow of Brain Pb were set for consistency with the brain retention curve predicted by the original model. The following transfer coefficients between plasma and brain were assigned:

$$\begin{aligned}\text{Plasma to Brain} &= 0.018 \text{ d}^{-1}, \\ \text{Brain to Plasma} &= 0.00095 \text{ d}^{-1}.\end{aligned}$$

The total outflow rate from plasma to all destinations combined in the ICRP model was left unchanged by reducing the transfer coefficients from plasma to each of the

compartments of *Other tissue* proportionally to their values in the ICRP model.

Alternate dose coefficients were derived for injection of  $^{210}\text{Pb}$  into blood of an adult male worker based on the systemic model for Pb applied in ICRP Publication 137 and the modified model with an explicitly modeled brain compartment described above. The dose coefficients for  $^{210}\text{Pb}$  included the contribution to dose from its radioactive progeny  $^{210}\text{Bi}$  and  $^{210}\text{Po}$  produced in the body after intake of  $^{210}\text{Pb}$ . Biokinetic models described in ICRP Publication 137 for radioisotopes of Bi and Po produced in systemic compartments by decay of a radioisotope of Pb were used together with the ICRP's model for Pb to derive one of the dose coefficients for brain. For calculation of the alternate dose coefficient based on explicit modeling of brain, the model for Bi as progeny of Pb applied in Publication 137 was modified by addition of a brain compartment with parameter values described above in the discussion of Bi. For  $^{210}\text{Po}$  produced in brain after intake of  $^{210}\text{Pb}$ , we applied the model for Po as Bi progeny applied in Publication 137, modified by addition of a brain pool as described above for Po. We examined the sensitivity of the dose coefficient for  $^{210}\text{Pb}$  to the alternate brain kinetics of Po considered earlier by deriving dose coefficients for  $^{210}\text{Pb}$  based on each set of parameter values (Brain Model A and Brain Model B described above).

The dose coefficient based on the modified model with an explicit brain compartment is 3.0 times the value based on the ICRP model if Brain Model A is applied to the progeny  $^{210}\text{Po}$ , and 3.5 times the value based on the ICRP models if Brain Model B is applied to  $^{210}\text{Po}$ .

## Plutonium

The ICRP's systemic model for plutonium (Pu) is updated in Part 4 of the series on occupational intake of radionuclides (to appear). See Leggett et al. (2005) for a description of that model including a list of transfer coefficients. As in previous ICRP biokinetic models for systemic Pu, the brain is included implicitly in *Other tissue*.

The U.S. Transuranium and Uranium Registries (USTUR) has studied the distribution of Pu in tissues of former nuclear workers (Kathren and Tolmachev 2019). The activity of  $^{239}\text{Pu}$  in liver and skeleton has been measured routinely, and activity in brain has been measured in some subjects. As a central estimate (mean, median, or geometric mean) for these individuals, the brain contains ~0.2% as much  $^{239}\text{Pu}$  as liver and skeleton combined (Figure 6).

Uptake and retention of Pu by the brain has been measured in laboratory animals following its parenteral administration. In dogs, the ratio of activity in brain to that in the liver plus skeleton varied from about 0.00004 to 0.0023 at 13–30 d after injection, with a central value of about 0.0013 (mean, 0.0012; median, 0.0014) (Lloyd et al. 1976).

A modified version of the ICRP's model for systemic Pu was developed by adding a compartment representing brain and assigning flow rates between blood and brain consistent with the relative contents of Pu in brain and in liver + skeleton in Pu workers at late times and dogs at early times after

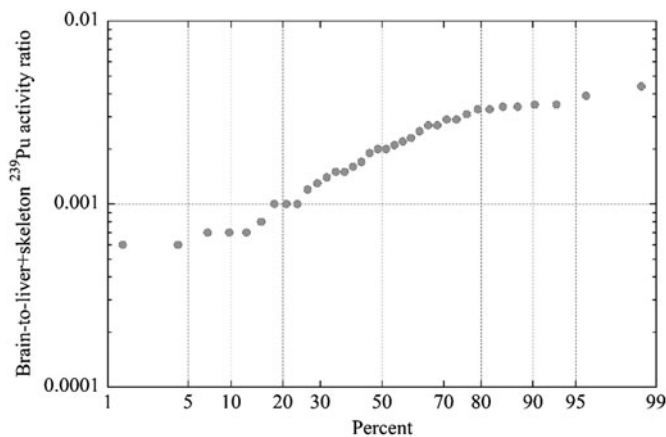


Figure 6. Brain activity of  $^{239}\text{Pu}$  relative to activity in liver plus skeleton in Pu workers.

exposure. The following transfer coefficients were assigned:

$$\begin{aligned}\text{Blood 1 to Brain} &= 0.0009 \text{ d}^{-1}, \\ \text{Brain to Blood 2} &= 0.0002 \text{ d}^{-1},\end{aligned}$$

where Blood 1 and Blood 2 are blood compartments that receive absorbed Pu and Pu returning from tissues to blood, respectively.

Dose coefficients were derived for brain for the case of injection of  $^{239}\text{Pu}$  into blood of a male worker, using the ICRP's systemic model for Pu and the modified version of that model with an explicit brain compartment. The dose coefficient based on the modified ICRP model with an explicit brain compartment is 0.96 times the value based on the ICRP model.

### Americium

The ICRP's systemic model for americium (Am) is updated in Part 4 of the series on occupational intake of radionuclides (to appear). The updated model is a modified version of the ICRP's model for systemic Am for adult members of the public adopted in Publication 67 (1993). The main changes from the earlier model are an added liver compartment and depiction of redeposition onto local cortical bone surface of a portion of the Am removed from cortical bone surface by bone restructuring processes. As in previous ICRP models for systemic Am, the brain is included implicitly in *Other tissue* in the updated model.

The USTUR whole-body analyses include a subject who apparently was exposed to pure  $^{241}\text{Am}$  about 25 y before his death (Breitenstein and Newton 1985; McInroy et al. 1985). The tissue of his left hand contained about 2% of the total-body content, suggesting that a puncture wound to his hand may have been the mode of exposure. The brain showed the lowest  $^{241}\text{Am}$  concentration of all systemic tissues. The concentration in brain was roughly 9% of the average concentration in soft tissues and 2% of the average concentration in the total body. The  $^{241}\text{Am}$  content in the brain represented about 0.037% of systemic  $^{241}\text{Am}$ . This is slightly below the lower end of the range of corresponding values for Pu indicated by USTUR data (Figure 6), assuming

that liver + skeleton represents at least 90% of systemic Pu at times remote from exposure.

Filipy and Kathren (1996) compared the concentrations of  $^{239+240}\text{Pu}$  and  $^{241}\text{Am}$  in brain and liver in each of eight USTUR donors with occupational exposures to these radionuclides. Much of the  $^{241}\text{Am}$  measured in these subjects may have arisen from production of  $^{241}\text{Am}$  in the body following intake of its parent  $^{241}\text{Pu}$ , which usually is found together with  $^{239}\text{Pu}$  and  $^{240}\text{Pu}$ . The concentration ratio  $^{239+240}\text{Pu}$ : $^{241}\text{Am}$  in liver ranged from 1.7 to 21, with mean and median values of  $10.6 \pm 6.4$  (SD) and 8.6, respectively. The mean and median concentration ratios of  $^{239+240}\text{Pu}$  in liver to that in brain were  $173 \pm 180$  (SD) and 105, respectively. The mean and median concentration ratios of  $^{241}\text{Am}$  in liver to that in brain were  $94 \pm 104$  (SD) and 55, respectively. The results suggest that the brain accumulates and/or retains Am to a lesser extent than Pu, particularly taking into account that the liver typically contains a much smaller portion of systemic Am than Pu at times remote from exposure, either in Pu workers or in subjects exposed directly to  $^{241}\text{Am}$ .

In baboons, the brain contained  $\sim 0.019\%$  of intravenously injected  $^{241}\text{Am}$  at 1–86 d after intravenous injection, 0.0081% at 206 d, and 0.0024% at 817 d (Guilmette et al. 1980). In dogs, the brain contained  $<0.001\%$  of intravenously administered  $^{241}\text{Am}$  at 1–22 d and 0.008% at 401–4448 d (Lloyd et al. 1970).

A modified version of the ICRP's model for systemic Am was developed by adding a compartment representing brain and assigning flow rates between blood and brain consistent with the relative contents of Am in brain and liver plus skeleton in human subjects at late times and in laboratory animals in the early months after exposure. The following transfer coefficients were assigned:

$$\begin{aligned}\text{Blood to Brain} &= 0.0024 \text{ d}^{-1}, \\ \text{Brain to Blood} &= 0.000077 \text{ d}^{-1}.\end{aligned}$$

Alternate dose coefficients were derived for brain for the case of injection of  $^{241}\text{Am}$  into blood of a male worker, using the ICRP's systemic model for Am and the modified version of that model with an explicit brain compartment. The dose coefficient based on the modified ICRP model with an explicit brain pool is 0.13 times the value based on the ICRP model.

### Cesium

A close physiological relationship of the alkali metals potassium (K), rubidium (Rb), and cesium (Cs) is well established. These elements compete for transport into and out of cells of the body with transport rates across cell membranes generally decreasing in the order  $\text{K} > \text{Rb} > \text{Cs}$  (Leggett et al. 2003).

The rate of transfer of K, Rb, or Cs from plasma into a tissue or organ can be estimated as the product of the blood flow rate to that tissue (plasma volumes per day) and an element- and tissue-specific extraction fraction, denoted by  $E_{T,X}$  for tissue T and element X, defined as the fraction of atoms extracted by that tissue in a single passage from arterial to venous plasma. The rate of return from a tissue to

plasma can be estimated from the relative contents of the element in plasma and the tissue at equilibrium as estimated from reported autopsy measurements for the element.

Experimentally determined tissue-specific extraction fractions typically are in the range 0.6–0.9 for K, 0.4–0.8 for Rb, and 0.05–0.2 for Cs for most tissues, but much lower extraction fractions are seen for the brain. Estimated extraction fractions for the brain are on the order of 0.015 for K, 0.01 for Rb, and 0.002 for Cs. For a reference adult male, the transfer coefficient describing flow of Cs, for example, from plasma into brain can be calculated as  $0.002 \times 0.12 \times 1766 \text{ d}^{-1} = 0.424 \text{ d}^{-1}$ , where 0.002 is the extraction fraction for brain for Cs, 0.12 is the reference fraction of cardiac output received by brain, and  $1766 \text{ d}^{-1}$  is the reference cardiac output in terms of the volume of plasma pumped through the heart each day. The transfer coefficient describing total outflow of Cs from brain is estimated as  $0.002 \times 0.424 \text{ d}^{-1} / 0.01 = 0.0848 \text{ d}^{-1}$  (corresponding to a half-time of  $\sim 8 \text{ d}$ , a relatively long half-time for escape of Cs from tissues), where 0.002 and 0.01 are reference fractions of total-body Cs in plasma and brain, respectively, at equilibrium, as estimated from reported autopsy measurements of concentrations of Cs in tissues of the adult human body. Based on these concepts, K, Rb, or Cs is estimated to be taken up much more slowly by the brain than by other tissues but also to be retained much longer by the brain than by other tissues.

These concepts were used to develop the ICRP's updated model for Cs described in ICRP Publication 137 (2017). The model was originally constructed around a framework representing the paths of blood flow in the human body (Leggett et al. 2003). The original model structure was later replaced by a more conventional model structure built around a central blood pool (Leggett, 2014). The latter structure was used in ICRP Publication 137.

A modified version of the model for systemic Cs used in ICRP Publication 137 was developed for this study by eliminating the brain compartment and increasing the deposition fractions in the compartments of *Other tissue* so that deposition fractions for all tissues and excretion pathways still add to 1.0.

Alternate dose coefficients were derived for the case of injection of  $^{134}\text{Cs}$  into blood of a male worker, using the ICRP's systemic model for Cs and the modified version of that model with brain implicitly contained in *Other tissue*. The dose coefficient based on the ICRP model with an explicit brain compartment is 1.5 times the value based on the modified model.

## Manganese

Manganese (Mn) is an essential trace element required for metabolism of amino acids, proteins, carbohydrates, and lipids in mammals. Ingested Mn is absorbed from the gut via the portal vein and is removed by the liver as required to achieve homeostasis. Manganese entering blood by other routes, for example, by absorption from the lungs after inhalation, initially bypasses the control processes in the liver and ultimately becomes largely bound to transferrin, which may

be transferred to the brain or other tissues by transferrin receptors. Thus, intake of Mn by routes other than ingestion affect its biokinetics and homeostatic balance and result in elevated accumulation in the brain. Excessive inhalation of Mn can result in adverse health effects including progressive neurodegenerative damage with an associated motor dysfunction syndrome similar to that seen in Parkinson's disease. Most reported cases of Mn intoxication have been linked to chronic occupational exposure to airborne Mn, particularly among manganese miners, welders, smelters, and workers in dry cell battery factories (Leggett 2011).

Isotopic studies on laboratory animals show that absorbed or intravenously injected manganese leaves blood rapidly and initially concentrates mainly in organs rich in mitochondria, particularly the liver, pancreas, and kidneys. Over time, other organs, especially brain and bone, contain increasingly larger portions of the retained activity. Studies on rats indicate that for most tissues the concentration as a function of time roughly paralleled whole-body retention, but bone and brain had slower loss than other tissues (Leggett 2011). The adult human brain has been estimated to contain about 5% of the total body content of stable manganese.

The ICRP's latest biokinetic model for Mn is described briefly in ICRP Publication 134 (2016b), where the model is used to describe the behavior of Mn as a progeny of iron (Fe). A more detailed description including a figure showing the model structure and a table of transfer coefficients can be found in an article by Leggett (2011). The model was developed from data on the time-dependent behavior of Mn in human subjects and laboratory animals, together with autopsy studies of the distribution of Mn in the human body. The model contains a compartment explicitly representing the brain. As depicted in the model, the brain takes up only 0.1% of the outflow of Mn from blood plasma following its inhalation and absorption to blood, but the retention time is much longer in the brain than in other soft tissues, resulting in a gradual increase in the Mn concentration in brain relative to other soft tissues.

A modified version of the ICRP's model for systemic Mn was developed by eliminating the brain compartment and increasing the deposition fractions in the compartments of *Other tissue* so that deposition fractions for all tissues and excretion pathways still add to 1.

Alternate dose coefficients were derived for the case of injection of  $^{54}\text{Mn}$  into blood of a male worker, using the ICRP's systemic model for Mn and the modified version of that model with brain implicitly contained in *Other tissue*. The dose coefficient based on the ICRP model with an explicit brain pool is 1.7 times the value based on the modified model.

## Mercury vapor

Inhaled mercury (Hg) vapor is carried in plasma to tissues including the brain, where it readily crosses the blood–brain barrier. After entering brain tissue, Hg vapor is oxidized to the divalent form of Hg, which is trapped in the brain because it is difficult for the divalent form to cross the



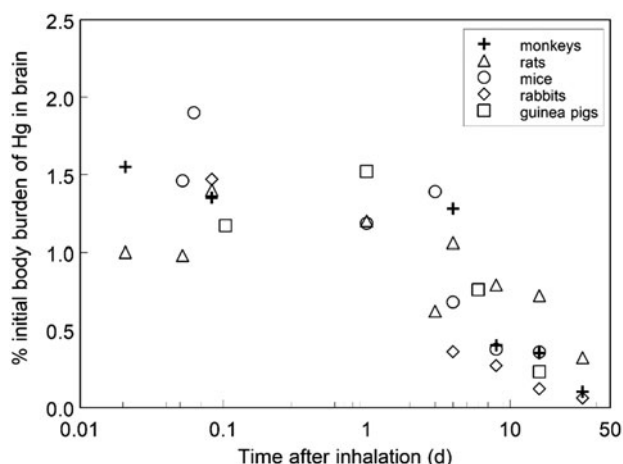


**Figure 7.** Observations of time-dependent content of Hg in the brain in laboratory animals after acute inhalation of Hg vapor. Data from Khayat and Dencker 1983, 1984; Magos 1967; Berlin et al. 1969; Nordberg and Serenius 1969; Hursh et al. 1976.

blood–brain barrier. Studies on mice, rats, rabbits, and monkeys indicate that fractional uptake of mercury by the brain is an order of magnitude greater after inhalation of Hg vapor than after intravenous injection of Hg salts (Berlin et al. 1966, 1969).

After acute inhalation of Hg vapor by squirrel monkeys, rats, mice, rabbits, and guinea pigs, the peak mercury content in the brain typically was 1–2% of the initial body burden (Figure 7). The pattern of uptake and retention was broadly consistent across species, despite the large variation in brain size as a fraction of total body weight in the studied species. The data for laboratory animals indicate a biological half-time on the order of 10 d for the preponderance of inorganic Hg deposited in the brain. Estimates of the removal half-time of Hg from the brain in human subjects exposed to Hg vapor or divalent Hg are in the range 14–29 d (Hursh et al. 1976; Newton and Fry 1978).

A long-term component of retention of Hg in the brain is suggested by some studies on laboratory animals and by autopsy data for human subjects who were occupationally exposed to Hg vapor. Studies involving acute exposure to laboratory animals suggest that long-term retention (weeks) of Hg in the brain following inhalation of Hg vapor represents at most 2% of the inhaled amount.

A provisional biokinetic model for systemic Hg applicable to different forms of inorganic Hg including Hg vapor has been developed for the ICRP's OIR series. The model structure is shown in Figure 8. Parameter values are not yet available in ICRP reports or in the open literature and hence are provided here (Table 2).

A modified version of the ICRP's provisional model for systemic Hg vapor was developed by eliminating the two brain compartments and increasing the deposition fraction in the compartment of *Other tissue* named *Other 1*, so that deposition fractions for all tissues and excretion pathways still add to 1.

Alternate dose coefficients were derived for the case of injection of  $^{203}\text{Hg}$  vapor into blood of a male worker, using the provisional ICRP model for Hg and the modified version of that

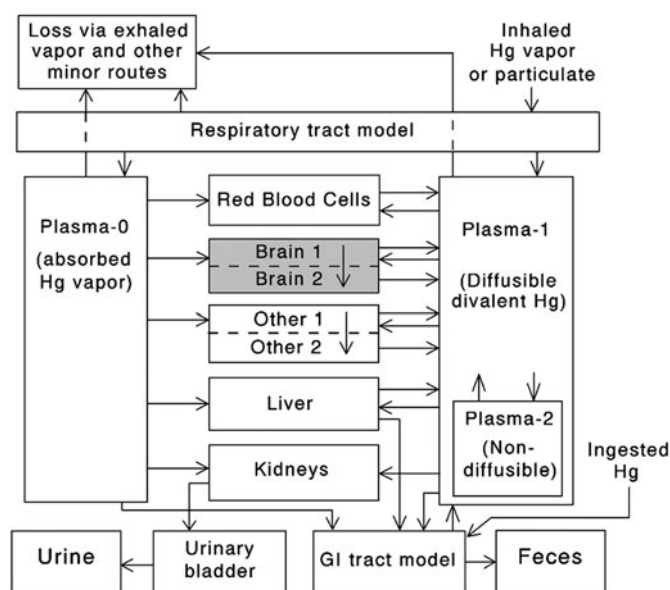


**Figure 8.** Structure of the ICRP's provisional model for mercury taken into the body as Hg vapor or divalent Hg.

**Table 2.** Transfer coefficients in the ICRP's provisional model for vapor and divalent forms of inorganic mercury.

Path	Transfer coefficient ( $\text{d}^{-1}$ )
Plasma-0 (Hg vapor) to:	
Red blood cells	100
Brain 1	20
Kidneys	120
Liver	50
Other 1	560
SI content	80
Minor excretion pathways	70
Plasma 1 (Diffusible divalent Hg) to:	
Red Blood Cells	0.665
Plasma 2 (Nondiffusible divalent Hg)	1.996
Brain 1	0.0333
Kidneys	5.823
Liver	3.322
Other 1	2.296
Small intestine content	1.664
Minor excretion pathways	0.832
Red Blood Cells to Plasma 1	0.231
Plasma 2 to Plasma 1	0.693
Brain 1 to Plasma 1	0.0329
Brain 1 to Brain 2	0.00173
Brain 2 to Plasma 1	0.000380
Kidneys to Urinary bladder content	0.0198
Liver to Small intestine content	0.0347
Liver to Plasma 1	0.0347
Other 1 to Plasma 1	0.0260
Other 1 to Other 2	0.00866
Other 2 to Plasma 1	0.00693

model with brain implicitly contained in *Other tissue*. The dose coefficient based on the ICRP model with an explicit brain pool is 1.4 times the value based on the modified model.

## Radium

The ICRP's systemic model for radium was updated in ICRP Publication 137 (2017). The updated model is a modified version of the ICRP's model for systemic Ra for adult members of the public adopted in Publication 67 (1993). The main changes from the earlier model are an added liver

compartment and compartments explicitly representing the kidneys. As in previous ICRP models for systemic Ra, the brain is included implicitly in *Other tissue*.

Schlenker et al. (1982) reviewed autopsy data on the  $^{226}\text{Ra}$  content of soft tissues in 17 subjects who received  $^{226}\text{Ra}$  by injection or ingestion at times from 5 d to 53 y before death. Schlenker and coworkers normalized  $^{226}\text{Ra}$  concentrations to total body activity. That is,  $^{226}\text{Ra}$  concentrations in tissues were tabulated as specific activity in individual tissues divided by total body activity. Data for brain were given for four times or time periods post injection: 230–1800 d; 4200 d; 17,000 d; and 17,700 d. Comparison of the normalized activity in brain to corresponding values for other sampled tissues contained in *Other tissue* in the ICRP's model for Ra suggest that the normalized concentrations in brain may be about 1.5–3.0 times higher than the median normalized concentration in *Other tissue*, depending on the time after intake and the method of deriving the median concentration in *Other tissue* from the uneven data set. The median value was used here as the measure of central tendency in view of the wide scatter in normalized concentrations for soft tissues.

Following intravenous administration of  $^{224}\text{Ra}$  chloride to dogs, the activity in brain expressed as a percentage of total activity in soft-tissues excluding liver and kidneys (i.e. in *Other tissue* in the ICRP's model for systemic Ra) increased continually with time over the 7-d observation period: 0.07% at 1 h, 0.13% at 8 h, 0.28% at 1 d, 0.61% at 3 d, and 1.43% at 7 d.

A modified version of the ICRP's model for systemic Ra was developed by adding a compartment representing brain and assigning transfer rates between plasma and the brain compartment that yield model predictions reasonably consistent with the data for human subjects at times remote from exposure and the data for dogs at early times after injection. The following transfer coefficients between blood and brain were assigned:

$$\begin{aligned}\text{Blood to Brain} &= 0.0035 \text{ d}^{-1}, \\ \text{Brain to Blood} &= 0.00038 \text{ d}^{-1}.\end{aligned}$$

The transfer coefficient from brain to blood is the value applied to the slow turnover compartment of *Other tissue* in the ICRP model. The total outflow rate from plasma to all destinations combined was left unchanged by reducing the transfer coefficient from the slow turnover compartment of *Other tissue* by the transfer coefficient from blood to brain.

Alternate dose coefficients were derived for brain for the case of injection of  $^{226}\text{Ra}$  into blood of a male worker, using the ICRP's systemic model for Ra and the modified version of that model with an explicit brain compartment. For simplicity, attention was restricted to dose from the parent radionuclide  $^{226}\text{Ra}$  only, which contributes more than 90% of the dose to brain in the ICRP's model. The dose coefficient based on the modified ICRP model with an added explicit brain pool is 1.9 times the value based on the ICRP's unmodified model.

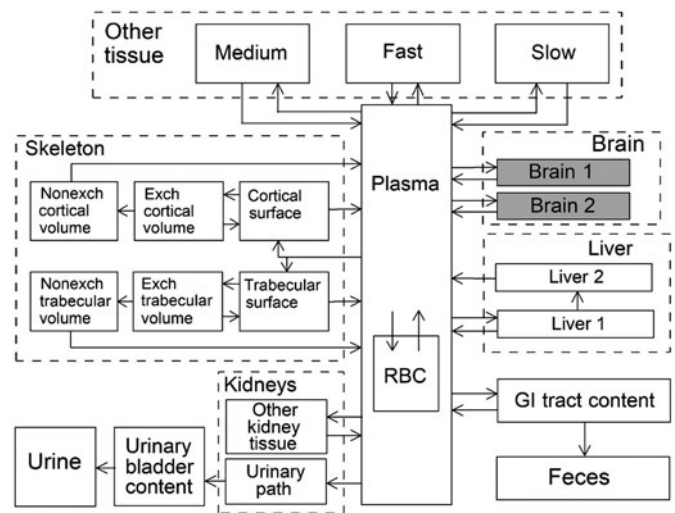


Figure 9. Model structure for systemic U. The unshaded boxes and associated arrows represent the ICRP's latest model (ICRP2017). The modified version of the ICRP model considered here adds two brain compartments and associated arrows. RBC: red blood cells; Exch: exchangeable; Nonexch: nonexchangeable; GI: gastrointestinal.

### Uranium

The ICRP's systemic model for uranium is described in ICRP Publication 137 (2017). The model structure is shown in Figure 9. In this model, the brain is included implicitly in *Other tissue*.

The tissue distribution of uranium was determined in three USTUR donors (Registrants) thought to have only environmental exposure to U (Kathren and Tolmachev 2015) and in two Registrants with occupational exposure to U (Russell and Kathren 2004; Avtandilashvili et al. 2015). The U content of brain as a percentage of systemic U was 0.4–1.0% in the environmentally exposed subjects and 0.4–1.2% in the occupationally exposed subject. The average for the five subjects was 0.7%.

Six months after surgical implant of depleted uranium pellets into rats, an unexpectedly high, dose-dependent accumulation of U was observed in the rat brain (Pellmar et al. 1999). Uranium was found to be heterogeneously distributed in the brain.

Rats exposed repeatedly over 3 weeks to depleted uranium dioxide via inhalation showed U concentrations in brain substantially higher than control animals. The concentration in different regions of the brain at 1 d after the end of exposure decreased in the order: olfactory bulb > hippocampus > frontal cortex > cerebellum (Monleau et al. 2005). The U concentration in all four regions decreased to control values over the next few days.

At 5 y after inhalation of uranium oxide by dogs, the average concentration of uranium in bone was about 2200 times that in brain (Tikhaya et al. 1965). The average concentrations in liver, kidneys, and spleen were, respectively, 73, 45, and 35 times that in brain.

A modified version of the ICRP's model for systemic U was developed by adding two compartments representing brain (Figure 9) and assigning transfer coefficients between plasma and these compartments that yield model predictions

reasonably consistent with the data for human subjects and laboratory animals. The following transfer coefficients between plasma and brain compartments were assigned:

$$\begin{aligned}\text{Plasma to Brain 1} &= 0.0326 \text{ d}^{-1}, \\ \text{Plasma to Brain 2} &= 0.00147 \text{ d}^{-1}, \\ \text{Brain 1 to Plasma} &= 0.0347 \text{ d}^{-1}, \\ \text{Brain 2 to Plasma} &= 0.000019 \text{ d}^{-1}.\end{aligned}$$

The outflow rates from Brain 1 and Brain 2 to plasma were assumed to be the same as the outflow rates from the medium and slow exchange compartments of *Other tissue* in the ICRP's systemic model for U. The total outflow rate from plasma to all destinations combined was left unchanged by reducing the transfer coefficients from plasma to the medium and slow exchange compartments of *Other tissue* proportionally to their values in the ICRP model.

Alternate dose coefficients were derived for brain for the case of injection of  $^{234}\text{U}$  into blood of a male worker, using the ICRP's systemic model for U and the modified version of that model with explicit brain compartments. The dose coefficient based on the modified ICRP model with an explicit brain pool is 0.81 times the value based on the ICRP model.

## Summary and conclusions

Typically, an element-specific systemic biokinetic model used in dose reconstruction for a radionuclide depicts explicitly only the dominant repositories of the element. Remaining tissues are aggregated into a pool called *Other tissue* in which the element is assumed to be uniformly distributed.

In the systemic biokinetic models currently used in dose reconstructions, the brain usually is addressed as an implicit mass fraction of *Other tissue* rather than an explicitly depicted repository. Due to increasing interest in potential adverse effects of radiation on the brain, efforts are underway within the Million Person Study to improve brain dosimetry for both internal and external radiation sources (Boice et al. 2006, 2014; Ellis et al. 2018). As part of this effort, we are assessing potential improvements in brain dosimetry for internal emitters resulting from explicit modelling of brain kinetics rather than treating the brain as an implicit mass fraction of *Other tissue*. This paper summarizes results of 10 case studies in which we compared dose coefficients for the brain based on two versions of the ICRP's latest model for the radionuclide of interest. If the ICRP model contained an explicit brain pool, we built an alternate version of the model depicting brain as a mass fraction of *Other tissue*. If the ICRP model included brain in *Other tissue*, we built an alternate version of the model that included an explicit brain pool with kinetics based on best available brain-specific data.

The results of the study are summarized in Table 3. The values in the right column of Table 3 are ratios A:B, where A is the dose coefficient based on the version of the model with an explicit brain pool, and B is the dose coefficient based on the version of the model in which the brain is implicitly contained in *Other tissue*. It is assumed in each case that the radionuclide is injected into blood of an adult male worker.

**Table 3.** Summary of ratios of injection dose coefficients for brain in a reference male worker, based on systemic biokinetic models with or without an explicitly modeled brain.

Radionuclide	Ratio of dose coefficients for brain	
	Explicit Brain	Implicit Brain
Americium-241		0.13
Bismuth-207		0.57
Uranium-234		0.81
Plutonium-239		0.96
Mercury-203 (vapor)		1.4
Cesium-134		1.5
Manganese-54		1.7
Polonium-210		1.7 <sup>a</sup>
Radium-226		1.9 <sup>b</sup>
Lead-210		3.3 <sup>c</sup>

<sup>a</sup>Average ratio. Alternate explicit brain models were addressed (see text).

<sup>b</sup>Based on dose from  $^{226}\text{Ra}$  only; contribution from progeny not considered.

<sup>c</sup>Average ratio. Alternate explicit brain models were addressed for  $^{210}\text{Po}$  produced in the body after intake of  $^{210}\text{Pb}$  (see text).

Based on reviews of biokinetic data for brain for the present case studies and for additional elements not addressed here, it appears that the brain typically has a lower rate of uptake per gram of tissue but a longer residence time than do most other studied soft tissues. Thus, an initially low uptake of a radionuclide by brain should not be interpreted as indicating that the dose to brain is smaller than that of most other tissues.

For the 10 radionuclides addressed in this study, the ratio A:B defined above ranged from 0.13 to 3.3 and were in the range 1.4–3.3 in six of the 10 case studies. This indicates that a dose estimate for brain based on a biokinetic model with brain implicitly contained in *Other tissue* may substantially underestimate or substantially overestimate a dose estimate that reflects best available brain-specific biokinetic data.

Regarding those radionuclides addressed here that are frequently encountered in the MPS, the results of this study indicate that addition of an explicit brain model in the current systemic models for U and Pu does not appear to be needed for epidemiological purposes because this would result in little change in dose estimates for brain for important isotopes of these elements. Addition of an explicit brain model to current systemic models for Po, Ra, and Am does appear to be warranted at least for epidemiological purposes because best available data suggest that the current models may substantially over- or underestimate the dose to brain from important isotopes of these elements.

In interpreting the results of the study as summarized in Table 3, it should be kept in mind that the 10 elements were not selected entirely at random. Four of the elements (Mn, Cs, Hg, and Pb) were chosen for convenience, in that the latest ICRP models for these elements (or a more detailed, published version of the latest ICRP model, in the case of Pb) already included an explicit brain pool. This helped to minimize biokinetic modeling efforts in the study. Of the four elements with existing brain models, three (Mn, Hg as vapor, and Pb) are known to have relatively high uptake by the brain. Thus, regarding the ratio A:B of dose coefficients for brain based on biokinetic models with or without explicit brain pools, the overall results of this study are biased on the high side.

For a given radionuclide, the potential for improvement of dose estimates for brain through explicit depiction of the brain in the systemic model depends on the quantity and quality of available element-specific biokinetic data for brain and the associated uncertainties in a predictive brain model based on those data. Ideally, only data for human subjects would be used in the development of a biokinetic model for humans. In practice, it is often necessary to supplement data for human subjects with findings for laboratory animals and in some cases to rely solely on animal data. The reader is referred to an article by Leggett (2001) for a critical examination of the basis for interspecies extrapolation of biokinetic data, the sources and extent of uncertainties inherent in such extrapolation, and the preferred animal species to use as laboratory models for different families of elements.

The preponderance of published data on accumulation of elements in the brain come from studies on laboratory animals. Best available data for the human brain generally come from autopsy studies of occupationally or environmentally exposed subjects. Such autopsy data were found for seven of the elements addressed here: Cs, Mn, Pb, Ra, U, Pu, Am. The brain models applied here to these elements were required to be consistent with the element-specific brain contents (as a percentage of the systemic content) determined in the autopsy studies. The brain model for Cs is a well-supported model based on data on the blood perfusion rate in the human brain and measurements of the fraction of blood-borne Cs extracted by the brain during passage of blood through the brain, in addition to autopsy measurements of environmental  $^{137}\text{Cs}$  in human tissues including brain. For Mn, Pb, Ra, U, Pu, and Am, data for laboratory animals were used to model the rate of accumulation in the brain starting at the beginning of exposure. For radioisotopes of these six elements addressed here ( $^{54}\text{Mn}$ ,  $^{210}\text{Pb}$ ,  $^{226}\text{Ra}$ ,  $^{234}\text{U}$ ,  $^{239}\text{Pu}$ , and  $^{241}\text{Am}$ ), analyses were performed to determine the sensitivity of the dose coefficients for brain, based on explicitly depicted brain models, to uncertainties in the interspecies extrapolation of the data. It was found that the dose estimates for brain were largely determined by the requirement that predictions of the brain model be consistent with the results of the autopsy data. Stated differently, the dose coefficients for brain for  $^{54}\text{Mn}$ ,  $^{210}\text{Pb}$ ,  $^{226}\text{Ra}$ ,  $^{234}\text{U}$ ,  $^{239}\text{Pu}$ , and  $^{241}\text{Am}$  based on explicit brain models were found to be only moderately sensitive to uncertainties (within reasonable uncertainty bounds) in the use of animal data to predict brain kinetics of the element at early times after intake. For example, if the rate of uptake of  $^{239}\text{Pu}$  by the brain was varied within a factor of 2 of the value indicated by data for dogs and the biological half-time in the brain was covaried so that model predictions remained consistent with USTUR autopsy data, the derived committed dose to the human brain varied within 20% of the value based on the explicit brain model applied here to  $^{239}\text{Pu}$ .

The most problematic data set underlying any of the brain models applied in this analysis is the collection of information for bismuth, consisting of data for rats and autopsy data for patients who had received Bi treatments. The value of the autopsy data is limited by a lack of information on

the time frame between Bi intake and death, the state of health of the subjects, and the possibility of a mass effect on the biokinetics of Bi due to the relatively high masses of administered Bi. The rat is not the preferred laboratory model for human biokinetics of elements and may be a particularly poor model for human brain kinetics in view of a variety of differences between rats and humans including brain size compared with total body size.

The behavior of inhaled Hg vapor has been studied extensively in laboratory animals, and some data are available from controlled studies on human subjects. The collective data provided a relatively strong foundation for development of the model for Hg vapor applied in this paper.

The construction of the brain model for Po differed from those of the other elements addressed here in that data for humans were not used. This was due to the difficulty in interpreting available autopsy data for  $^{210}\text{Po}$  as the subjects were also exposed not only to  $^{210}\text{Po}$  but also to radionuclides that sequentially decayed to  $^{210}\text{Po}$  *in vivo* (Blanchard and Moore 1971) and concern that accumulation of  $^{210}\text{Po}$  in brain of a subject who died from  $^{210}\text{Po}$  poisoning did not reflect typical brain kinetics of Po (Harrison et al. 2017). Data on  $^{210}\text{Po}$  kinetics in baboons were judged to be the most relevant data for modeling brain kinetics of Po in humans. Alternate methods of extrapolation of Po uptake data by brain were considered. It was assumed that the residence time of Po in the brain is the same in baboons and humans, which is another source of uncertainty in the application of baboon data to humans. The baboon data seem more likely to underestimate than overestimate the residence time of Po in the brain in humans in view of a moderately shorter residence time of Po in baboons (Leggett and Eckerman 2001). In any case, the present analysis for  $^{210}\text{Po}$  suggests that inclusion of brain in *Other tissue* is likely to result in an underestimate of the dose to the brain from internally deposited  $^{210}\text{Po}$ .

## Disclosure statement

The authors declare no conflict of interest. The authors alone are responsible for the content and writing of the paper.

## Funding

This manuscript and research were supported by UT-Battelle, LLC under Contract No. DE-AC05-00OR22725 with the U.S. Department of Energy. The United States Government retains and the publisher, by accepting the article for publication, acknowledges that the United States Government retains a non-exclusive, paid-up, irrevocable, world-wide license to publish or reproduce the published form of this manuscript, or allow others to do so, for United States Government purposes. The U.S. Department of Energy will provide public access to these results of federally sponsored research in accordance with the DOE Public Access Plan (<http://energy.gov/downloads/doe-public-access-plan>). The work described in this manuscript was sponsored by the U.S. Department of Energy under WAS Project No. 2018-AU-2000MPS, the U.S. Department of Energy, Office of Domestic and International Health Studies (AU-13), under grant award number DE-HS0000073 (USTUR funding), the Centers for Disease Control and Prevention (CDC) Office of Noncommunicable Diseases, Injury and Environmental Health, National Center for Environmental Health, under Interagency Agreement DOE No. 2220-



Z051-16, under contract No. DE-AC05-00OR22725 with UT-Battelle, nd under grant No. 5NUE1EH001315 with the National Council on Radiation Protection and Measurements (NCRP). The authors also are grateful for the financial support received by the NCRP from the U.S. Department of Energy (Grant No. DE-AU0000042) and from the National Aeronautics and Space Administration (Grant No. 80NSSC17M0016).

## Notes on contributors

**Richard W. Leggett** is a research scientist in the Environmental Sciences Division at Oak Ridge National Laboratory (ORNL). His main research interest is in physiological systems modeling, with primary applications to the biokinetics and dosimetry of radionuclides and radiation risk analysis. He is a member of Committee 2 of the International Commission on Radiological Protection (ICRP) and the ICRP Task Group on Internal Dose Coefficients (IDC). His physiological systems models of the human circulation, skeleton, and gastrointestinal transfer and his systemic biokinetic models for many elements are used by the ICRP as dosimetry and bioassay models. He is the author of ICRP Publication 70, Basic Anatomical and Physiological Data for Use in Radiological Protection: The Skeleton, and co-author of several other ICRP reports.

**Sergei Y. Tolmachev** is Associate Research Professor in the College of Pharmacy and Pharmaceuticals Sciences (COP), Washington State University, where he directs the U.S. Transuranium and Uranium Registries Research Center and the National Human Radiobiology Tissue Repository. His current research interests are in the area of radiation protection, including radionuclide biokinetic modelling, actinide decorporation treatment, retrospective biodosimetry, and study of radioactive nanoparticles as well as application of mass-spectrometric techniques for stable element determination in the human body.

**John D. Boice** is President of the National Council on Radiation Protection and Measurements and Professor of Medicine at Vanderbilt University. He is an international authority on radiation effects and served on the Main Commission of the International Commission on Radiological Protection and on the United Nations Scientific Committee on the Effects of Atomic Radiation. He directs the Million Person Study of Low-Dose Health Effects.

## References

- Avtandilashvili M, Puncher M, McComish SL, Tolmachev SY. 2015. US Transuranium and Uranium Registries case study on accidental exposure to uranium hexafluoride. *J Radiol Prot.* 35:129–151.
- Berlin M, Fazackerley J, Nordberg G. 1969. The uptake of mercury in the brains of mammals exposed to mercury vapor and to mercuric salts. *Arch Environ Health.* 18:719–729.
- Berlin M, Jerksell LG, von Ubsich H. 1966. Uptake and retention of mercury in the mouse brain. A comparison of exposure to mercury vapor and intravenous injection of mercuric salt. *Arch Environ Health.* 12: 33–42.
- Blanchard RL, Moore JB. 1971. Body burden, distribution and internal dose of  $^{210}\text{Pb}$  and  $^{210}\text{Po}$  in a uranium miner population. *Health Phys.* 21:499–518.
- Boice JD. 2017. Space: the final Frontier-Research Relevant to Mars. *Health Phys.* 112:392–397.
- Boice JD, Jr, Cohen SS, Mumma MT, Ellis ED, Cragle DL, Eckerman KF, Wallace PW, Chadda B, Sonderman JS, Wiggs LD. 2014. Mortality among Mound workers exposed to polonium-210 and other sources of radiation, 1944–1979. *Radiat Res.* 181:208–228.
- Boice JD, Ellis ED, Golden AP, Girardi DJ, Cohen SS, Chen H, Mumma MT, Shore RE, Leggett RW. 2018. The past informs the future: an overview of the Million Worker Study and the Mallinckrodt Chemical Works Cohort. *Health Phys.* 114:381–385.
- Boice JD, Jr, Leggett RW, Ellis ED, Wallace PW, Mumma M, Cohen SS, Brill AB, Chadda B, Boecker BB, Yoder RC, et al. 2006. A comprehensive dose reconstruction methodology for former Rocketdyne/Atomics International radiation workers. *Health Phys.* 90:409–430.
- Breitenstein BD, Newton CE. 1985. Part I: Introduction and history of the case. In: *Health Phys.* 49, Special issue on The U.S. Transuranium Registry report on the Am-241 content of a whole body; 565–567.
- Bryce-Smith D, Stephens R. 1983. Sources and effects of environmental lead. In: *Trace elements in health* (Rose J, ed). London: Butterworths, 83–131.
- Cohen N, Eisenbud M, Wrenn ME. 1970. The retention and distribution of lead-210 in the adult baboon. Progress report, radioactivity studies. New York: NYU Medical Center.
- Cohen N, Fellman AL, Hickman DP, Ralston LG, Ayres LS. 1989. Primate polonium metabolic models and their use in estimation of systemic radiation doses from bioassay data. Miamisburg, OH: Mound Laboratory.
- Ellis ED, Boice JD, Jr, Golden AP, Girardi DJ, Cohen SS, Mumma MT, Shore RE, Leggett RW, Kerr GD. 2018. Dosimetry is key to good epidemiology: workers at Mallinckrodt Chemical Works had seven different source exposures. *Health Phys.* 114:386–397.
- Fellman A, Ralston L, Hickman D, Ayres L, Cohen N. 1994. Polonium metabolism in adult female baboons. *Radiat Res.* 137:238–250.
- Filipy RE, Kathren RL. 1996. Changes in soft tissue concentrations of plutonium and americium with time after human occupational exposure. *Health Phys.* 70:153–159.
- Fowler BA, Vouk VB. 1986. Chapter 6, Bismuth. In *Handbook on the toxicology of metals*. Vol. II. Friberg L, Nordberg GF, Vouk VB, eds. New York: Elsevier, 117–129.
- Gilbert ES, Cragle DL, Wiggs LD. 1993. Updated analyses of combined mortality data for workers at the Hanford Site, Oak Ridge National Laboratory, and Rocky Flats Weapons Plant. *Radiat Res.* 136:408–421.
- Grandjean P. 1978. Regional distribution of lead in human brains. *Toxicol Lett.* 2:65–69.
- Gregus Z, Klaassen CD. 1986. Disposition of metals in rats: a comparative study of fecal, urinary, and biliary excretion and tissue distribution of eighteen metals. *Toxicol Appl Pharmacol.* 85:24–38.
- Guilmette RA, Cohen N, Wrenn ME. 1980. Distribution and retention of  $^{241}\text{Am}$  in the baboon. *Radiat Res.* 81:100–119.
- Harrison J, Fell T, Leggett R, Lloyd D, Puncher M, Youngman M. 2017. The polonium-210 poisoning of Mr. Alexander Litvinenko. *J Radiol Prot.* 37:266–278.
- Hursh JB, Clarkson TW, Cherian MG, Vostal JJ, Mallie RV. 1976. Clearance of mercury (Hg-197, Hg-203) vapor inhaled by human subjects. *Arch Environ Health.* 31:302–309.
- International Commission on Radiological Protection (ICRP). 1993. ICRP Publication 67. Age-Dependent Doses to Members of the Public from Intake of Radionuclides Part 2 Ingestion Dose Coefficients. Ann ICRP. 23 (3/4). Oxford: Pergamon Press.
- International Commission on Radiological Protection (ICRP). 2002. ICRP Publication 89. Basic anatomical and physiological data for use in radiological protection: reference values. Ann ICRP. 32 (3/4). Oxford: Pergamon Press.
- International Commission on Radiological Protection (ICRP). 2016a. ICRP Publication 133. The ICRP computational framework for internal dose assessment for reference adults - specific absorbed fractions. Ann ICRP. 45(2). London: Sage.
- International Commission on Radiological Protection (ICRP). 2016b. ICRP Publication 134. Occupational intake of radionuclides, Part 2. Ann ICRP. 45(3/4). London: Sage.
- International Commission on Radiological Protection (ICRP). 2017. ICRP Publication 137. Occupational intake of radionuclides, part 3. Ann ICRP. 46(3/4). London: Sage.
- Kathren RL, Tolmachev SY. 2015. Natural uranium tissue content of three Caucasian males. *Health Phys.* 109:187–197.
- Kathren RL, Tolmachev SY. 2019. The United States Transuranium and Uranium Registries (USTUR): A five-decade follow-up of plutonium and uranium workers. *Health Phys.* 116: 000–000.
- Khayat A, Dencker L. 1984. Organ and cellular distribution of inhaled metallic mercury in the rat and marmoset monkey (*Callitrix jacchus*): influence of ethyl alcohol pretreatment. *Acta Pharmacol et Toxicol.* 55:145–152.

- Khayat A, Dencker L. 1983. Whole body and liver distribution of inhaled mercury vapor in the mouse: Influence of ethanol and aminotriazole pretreatment. *J Appl Toxicol.* 3:66–74.
- Lee SP, Lim TH, Pybus J, Clarke AC. 1980. Tissue distribution of orally administered bismuth in the rat. *Clin Exp Pharmacol Physiol.* 7: 319–324.
- Leggett RW. 1993. An age-specific kinetic model of lead metabolism in humans. *Environ Health Perspect.* 101:598–616.
- Leggett RW. 2001. Reliability of the ICRP's dose coefficients for members of the public. 1. Sources of uncertainty in the biokinetic models. *Radiat Prot Dosimetry.* 95:199–213.
- Leggett RW. 2011. A biokinetic model for manganese. *Sci Total Environ.* 409:4179–4186.
- Leggett RW. 2013. Biokinetic models for radiocaesium and its progeny. *J Radiol Prot.* 33:123–140.
- Leggett RW, Eckerman KF. 2001. A systemic biokinetic model for polonium. *Sci Total Environ.* 275:109–125.
- Leggett RW, Eckerman KF, Khokhryakov VF, Suslova KG, Krahenbuhl MP, Miller SC. 2005. Mayak worker study: an improved biokinetic model for reconstructing doses from internally deposited plutonium. *Radiat Res.* 164:111–122.
- Leggett RW, Williams LR, Melo DR, Lipsztein JL. 2003. A physiologically based biokinetic model for cesium in the human body. *Sci Total Environ.* 317:235–255.
- Lemerrier V, Millot X, Ansoborlo E, Ménétrier F, Flury-Héard A, Rousselle C, Scherrmann JM. 2003. Study of uranium transfer across the blood-brain barrier. *Radiat Prot Dosimetry.* 105:243–245.
- Lloyd RD, Atherton DR, McFarland SS, Mays CW, Stevens W, Williams JL, Taylor GN. 1976. Studies of injected  $^{237}\text{Pu}(\text{IV})$  citrate in beagles. *Health Phys.* 30:47–52.
- Lloyd RD, Mays CW, Atherton DR, Bruenger FW. 1975.  $^{210}\text{Pb}$  studies in beagles. *Health Phys.* 28:575–583.
- Lloyd RD, Mays CW, Taylor GN, Atherton DR. 1970. Americium-241 studies in beagles. *Health Phys.* 18:149–156.
- Lloyd RD, Mays CW, Taylor GN, Atherton DR, Bruenger FW, Jones CW. 1982. Radium-224 retention, distribution, and dosimetry in beagles. *Radiat Res.* 92:280–295.
- Magos L. 1967. Mercury-blood interaction and mercury uptake by the brain after vapor exposure. *Environ Res.* 1:323–337.
- McInroy JF, Boyd HA, Eutsler BC, Romero D. 1985. The U.S. Transuranium Registry report of the  $^{241}\text{Am}$  content of a whole body. Part IV: Preparation and analysis of the tissues and bones. *Health Phys.* 49: 587–621.
- Monleau M, Bussy C, Lestaevél P, Houpert P, Paquet F, Chazel V. 2005. Bioaccumulation and behavioural effects of depleted uranium in rats exposed to repeated inhalations. *Neurosci Lett.* 390:31–36.
- Nathwani AC, Down JF, Goldstone J, Yassin J, Dargan PI, Virchis A, Gent N, Lloyd D, Harrison JD. 2016. Polonium-210 poisoning: a first-hand account. *Lancet.* 388:1075–1080.
- National Council on Radiation Protection and Measurements (NCRP). 2016. Potential for central nervous system effects from radiation exposure during space activities. Phase 1: overview. Commentary No. 25. Bethesda, MD: NCRP.
- Newton D, Fry FA. 1978. The retention and distribution of radioactive mercuric oxide following accidental inhalation. *Ann Occup Hyg.* 21: 21–32.
- Nordberg GF, Serenius F. 1969. Distribution of inorganic mercury in the guinea pig brain. *Acta Pharmacol Toxicol (Copenh).* 27:269–283.
- Pellmar TC, Fuciarelli AF, Ejnik JW, Hamilton M, Hogan J, Strocko S, Emond C, Mottaz HM, Landauer MR. 1999. Distribution of uranium in rats implanted with depleted uranium pellets. *Toxicol Sci.* 49:29–39.
- Petit TL, Alfano DP, LeBoutillier JC. 1983. Early lead exposure and the hippocampus: a review and recent advances. *NeuroToxicology.* 4: 79–94.
- Russell JJ, Kathren RL. 2004. Uranium deposition and retention in a USTUR whole body case. *Health Phys.* 86:273–284.
- Schlenker RA, Keane AT, Holtzman RB. 1982. The retention of  $^{226}\text{Ra}$  in human soft tissue and bone; implications for the ICRP 20 alkaline earth model. *Health Phys.* 42:671–693.
- Silver SR, Bertke SJ, Hein MJ, Daniels RD, Fleming DA, Anderson JL, Pinney SM, Hornung RW, Tseng CY. 2013. Mortality and ionising radiation exposures among workers employed at the Fernald Feed Materials Production Center (1951–1985). *Occup Environ Med.* 70: 453–463.
- Sollmann TA. 1957. Manual of pharmacology and its applications to therapeutics and toxicology. Philadelphia: W.B. Saunders Co.
- Sollmann T, Seifter J. 1942. Intravenous injections of soluble bismuth compounds: Their toxicity, and their sojourn in the blood and organs. *J Pharmacol Exp Ther.* 74:134–154.
- Tikhaya MG, Novikova AP, Parfenov YuD. 1965. Body distribution of uranium in dogs long periods after the inhalation of uranium oxide (in Russian). *Med. Radiol.* 10(10): 50–54.
- Wiggs LD, Johnson ER, Cox-DeVore CA, Voelz GL. 1994. Mortality through 1990 among white male workers at the Los Alamos National Laboratory: considering exposures to plutonium and external ionizing radiation. *Health Phys.* 67:577–588.
- Zidenberg-Cherr S, Parks NJ, Keen CL. 1987. Tissue and subcellular distribution of bismuth radiotracer in the rat: considerations of cytotoxicity and microdosimetry for bismuth radiopharmaceuticals. *Radiat Res.* 111:119–129.